Journal of Computing and Electronic Information Management
ISSN: 2413-1660 | Vol. 16, No. 2, 2025

Design and mechanical analysis of wall-climbing ROV adsorption structure

Xuqing Liu [1, *], Jie Yu [1], Xinzhu Li [1], Changqin Chen [1], Xiao Chen [1], Xin Deng [1,2]

[1] Oil Production Service Branch of CNOOC Energy Technology & Services Limited, Tianjin, China
[2] School of Mechanical Science and Engineering, Northeast Petroleum University, Daqing Heilongjiang, China
[*] **Corresponding author**: Xuqing Liu (Email: liuxq28@cnooc.com.cn)

Abstract: This paper studies the design and reliability of a wheeled walking structure based on electromagnets for remotely operated underwater vehicles (ROV). First, the walking structure is based on the traditional wheeled structure and combined with electromagnet adsorption technology. It has the advantages of high adsorption reliability, controllable adsorption strength, and convenient separation from the magnetic wall. In addition, the safety of the designed structure in different adjacent states is mechanically analyzed to obtain the minimum feasible adsorption force. At the same time, the influence of the current input of the electromagnet on the adsorption capacity is explored through simulation. Finally, a set of mechanical experiments are conducted to verify the effectiveness of the design scheme and obtain a set of feasible design schemes.

Keywords: ROV; Wheeled walking mechanism; Wall-climbing; Mechanical analysis; Electromagnet.

1. Introduction

The underwater robot is a mobile diving device designed for underwater observation and operation [1-5]. It is one of the advanced technical means for humans to explore and understand the ocean and is an important equipment support for a country to build maritime power. Among them, ROV is often used to inspect marine engineering structures due to its high technical maturity and wide application range, but it operates in a floating state and is easily disturbed by the external environment. A wall-climbing robot is a special robot that can complete operations under vertical walls or inclined walls. It can be assembled and coordinated with different working modules, has strong portability, and has a wide range of applications. Therefore, the research and development of ROVs with wall-climbing functions has become the focus of scholars and engineers at home and abroad.

The adsorption device of wall-climbing ROV generally has four adsorption methods: vacuum negative pressure adsorption, magnetic adsorption, thrust adsorption and bionic adsorption [6-8]. Vacuum adsorption is not limited by the wall material, but has high requirements for the wall flatness; although thrust adsorption has no requirements for the wall material and smoothness, it is difficult to control and has serious noise pollution; bionic adsorption has strong obstacle-crossing ability but the technology is not yet mature; magnetic adsorption has the advantages of large adsorption force and strong load capacity, but is limited by the wall material, and the permanent magnetic adsorption force cannot be adjusted. To overcome the above difficulties, the magnetic adsorption technology based on electromagnets came into being, which can adjust the adsorption force by controlling the input current.

In addition, the movement mode is also the focus of the design of wall-climbing ROV. Generally, there are three types of movement modes: crawler, multi-legged, and wheeled [9-10]. The crawler movement mode has strong load capacity and certain obstacle-crossing ability, but poor steering ability and slow movement speed; the multi-legged movement mode has strong obstacle-crossing ability but complex structure and difficult control; the wheeled movement mode has fast movement speed and high flexibility.

In summary, in order to avoid underwater detection problems, this paper designs a wall-climbing ROV based on electromagnetic adsorption, which ensures the flexibility of underwater operations and provides reliable wall-climbing capabilities.

2. ROV Structure Design

The wall-climbing ROV designed in this paper is shown in Fig.1.

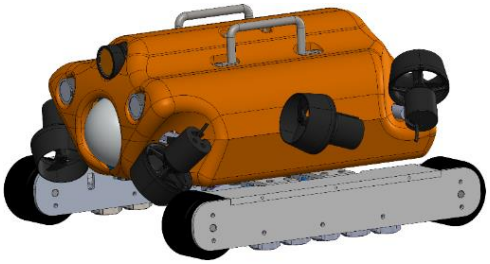

Fig.1 3D structure diagram of wall-climbing ROV

According to the modular parameterization concept, the robot studied can be divided into a buoyancy mechanism module, a thruster power module, a visual system module, a walking structure module, and a control cabin module. The ROV body structure adopts a streamlined design frame composed of plastic buoyancy materials. To improve the convenience of component installation and fixation and facilitate the processing of buoyancy materials, the buoyancy materials are manufactured in two parts, upper and lower. The control cabin is embedded in the middle of the buoyancy material, and the rotation and translation freedom of the cabin are limited by the metal skeleton. The control cabin module is the core module of the ROV, responsible for providing control signals for each component and transmitting power. The visual system module is responsible for target observation and positioning, and lighting is installed on both sides to ensure that the camera can still provide higher clarity in low-light environments.

The thruster power module is the power source for the robot's underwater movement and is responsible for controlling the robot's movement in the water. This ROV is equipped with 6 thrusters, four of which are mainly responsible for vertical movement and two for horizontal movement. The thrusters are fixed to the ROV at different angles to meet various posture requirements.

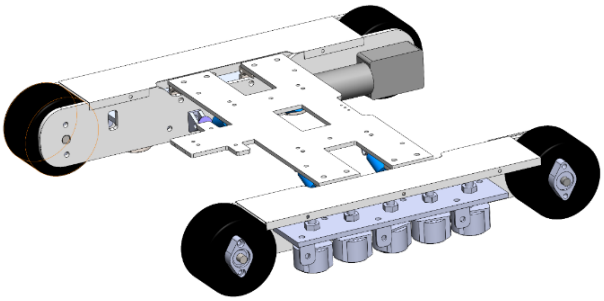

Fig.2 3D structure diagram of walking structure module

The walking structure module is shown in Fig .2, which adopts a wheeled structure. Considering the wall climbing function requirements, evenly distributed electromagnets are installed between the wheels on each side to provide adsorption force. The electromagnet has the high adsorption capacity of a permanent magnet and can be unloaded at any time to enhance flexibility. It should be pointed out that the electromagnet does not directly contact the ground or the magnetic wall surface, but controls the air gap between the ground and the magnetic wall surface through bolts, thereby maintaining a strong adsorption force while reducing friction loss.

3. Mechanical Analysis of ROV

The wall-climbing ROV has two operating modes: underwater and above water. Therefore, its operation on the offshore platform jacket (magnetic wall) can be simply classified into two situations, namely water operation and underwater operation. Compared with above-water operation, the ROV will be affected by its buoyancy when operating underwater, and the adsorption force required to stabilize on the magnetic wall is smaller. Therefore, in this section, we conduct a safety mechanical analysis on the two dangerous working conditions of sliding and longitudinal capsizing in the above-water operation and determine the minimum adsorption required by the electromagnet through different inclination angles and attitude angles.

3.1. Establishment of Spatial Posture

As shown in Fig .3, first consider the world coordinate system $O_W - X_W Y_W Z_W$, assuming that there is an arbitrary magnetic wall surface with an angle of α with plane $O_W - X_W Y_W Z_W$, and its coordinate system is $O_S - X_S Y_S Z_S$. An ROV is adsorbed on the magnetic wall surface, and its body coordinate system is $O_B - X_B Y_B Z_B$, and the angle with coordinate system $O_S - X_S Y_S Z_S$ is β .

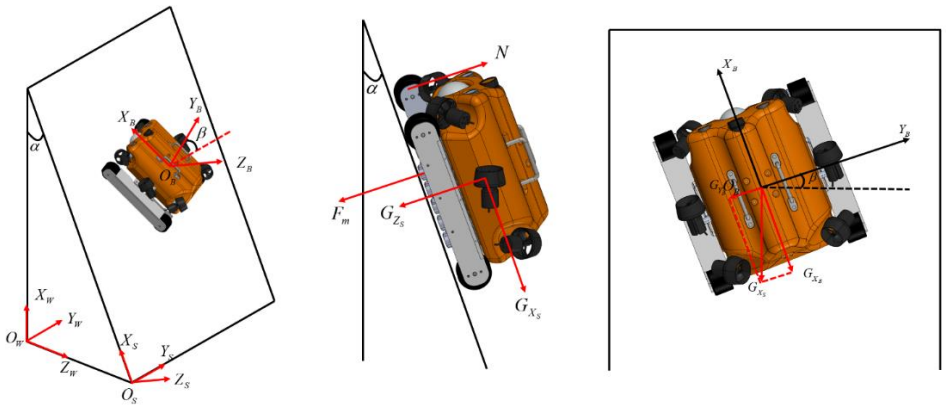

Fig.3 The spatial posture of ROV

As shown in Fig.3, the weight of ROV is represented by G . G can be decomposed in the coordinate system $O_S - X_S Y_S Z_S$ as follows:

$$\begin{cases} G_{X_S} = G\cos(\alpha) \\ G_{Z_S} = G\sin(\alpha). \end{cases} \tag{1}$$

Next, decompose G_{X_S} into coordinate system $O_B - X_B Y_B Z_B$ and obtain:

$$\begin{cases} G_{X_B} = G_{X_S}\cos(\beta) = G\cos(\alpha)\cos(\beta) \\ G_{Y_B} = G_{X_S}\sin(\beta) = G\cos(\alpha)\sin(\beta) \\ G_{Z_B} = G_{Z_S} = G\sin(\alpha). \end{cases} \tag{2}$$

To facilitate the following derivation, we introduce the following assumption: Considering the particularity of the electromagnetic adsorption wheeled walking structure proposed in this paper, we assume that the adsorption force of all electromagnets is the same and evenly distributed on the four wheels.

3.2. Slip safety analysis

When the ROV is stationary, the motor brake of the wheeled walking structure is closed. If the friction force is insufficient, the ROV may slide backward. Therefore, in order to prevent this phenomenon from happening, the following analysis is performed.

The support force N of a single wheel on the magnetic wall is:

$$N = \frac{10F_m + G_{Z_B}}{4} \tag{3}$$

where F_m is the adsorption force of a single electromagnet. Then the friction force f between the wheel and the magnetic wall is:

$$f = 4N\mu \tag{4}$$

where μ is the friction factor. Combining equations (2) and (4), we can see that to ensure that the ROV does not slide,

$f < G_{X_B}$ must be satisfied, that is:

$$F_m > \frac{G\cos(\alpha)\cos(\beta)}{10\mu} - \frac{G\sin(\alpha)}{10}. \tag{5}$$

3.3. Overturning safety analysis

When the ROV is stationary, it may also overturn along the $O_S Z_S$ axis at its lowest wheel. Only by ensuring that the uppermost wheel of the ROV does not separate from the magnetic wall can its safety be guaranteed. As shown in Fig.4, assume that the distance from the center of mass of the ROV along $O_B X_B$ to the lowest wheel is $\frac{L}{2}$, and the distance between the same side wheels of the wheeled walking mechanism is L; the vertical distance from the center of mass of the ROV to the magnetic wall is H.

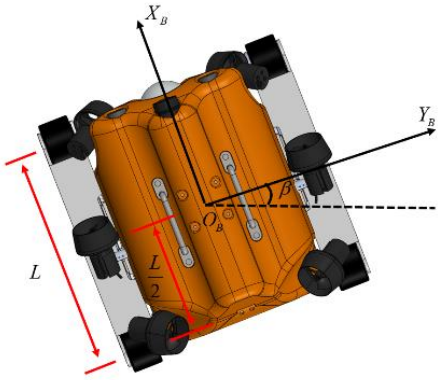

Fig.4 The overturning of ROV

According to the assumption, the suction force of the uppermost wheel is:

$$F_M = \frac{10F_m}{4} = \frac{5F_m}{2} \tag{6}$$

and the distance between the top wheel and the bottom wheel is known to be:

$$\bar{L} = \frac{L}{\cos(\beta)}. \tag{7}$$

According to equations (6) and (7), the anti-overturning moment M_p of ROV is:

$$M_p = F_M \bar{L} + G_{Z_B} \frac{\bar{L}}{2}. \tag{8}$$

When ROV is in a critical state of longitudinal rollover, the support force of the uppermost wheel is $N \to 0$, and the overturning moment is:

$$M_n = G_{X_S} H. \tag{9}$$

To ensure that the ROV does not slide by combining equations (8) and (9), it is necessary to meet the following requirements:

$$M_p > M_n \tag{10}$$

that is:

$$F_m > \frac{2GH\cos(\alpha)\cos(\beta)}{5L} - \frac{G\sin(\alpha)}{5}. \tag{11}$$

3.4. The solution of extreme values

Considering the characteristic that the adsorption force of the electromagnet cannot be negative, combining equations (5) and (11) can obtain the electromagnetic adsorption force that satisfies safety:

$$F_m = \max\{\frac{G\cos(\alpha)\cos(\beta)}{10\mu} - \frac{G\sin(\alpha)}{10}, \frac{2GH\cos(\alpha)\cos(\beta)}{5L} - \frac{G\sin(\alpha)}{5}, 0\}. \tag{12}$$

Based on the actual situation, we take $H = 150mm$, $\mu = 0.45$, $L = 470mm$, $G = 150N$. Calculate the relationship between F_m, α, and β separately, and obtain Fig.5 and Fig.6.

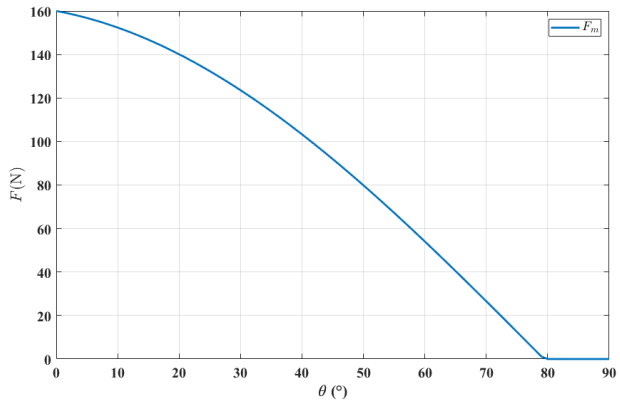

Fig.5 The trend of F_m changing with θ, when $\beta = 0$

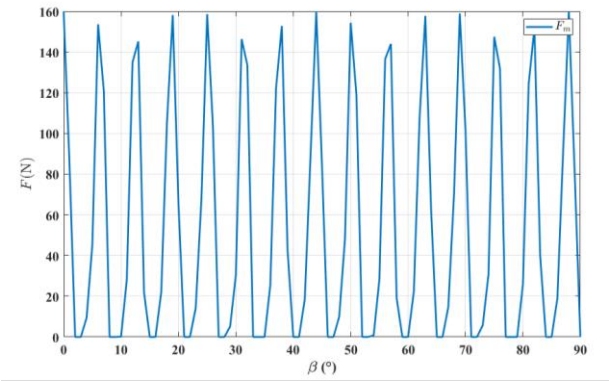

Fig.6 The trend of F_m changing with β, when $\alpha = 0$

Comparing Fig.5 and Fig .6, it can be seen that the minimum adsorption force required to ensure safety is $F_m = 160N$.

4. Analysis and simulation of adsorption capacity

The minimum adsorption force that ensures safety can be obtained through the analysis and calculation in the previous section. Meanwhile, the electromagnet is the core component of the wheeled walking structure proposed in this article, used to provide suction force. Therefore, this section will study the

adsorption force and influencing factors of the electromagnet.

4.1. Principle analysis

The working principle of an electromagnet is based on the magnetic effect of current. When current passes through a wire, a magnetic field is generated around it. If current passes through a solenoid, a uniform magnetic field is formed inside it. If a core is inserted into the center of the solenoid, the core will be magnetized and aligned with the direction of the solenoid's magnetic field, thereby enhancing its magnetism. Electromagnets are mainly composed of an iron core, coil, and armature. The iron core is usually made of soft iron or silicon steel to quickly demagnetize after power failure; The coil is wound around the outside of the iron core, generating a magnetic field through current. When the number of coils and the size of the magnet are fixed, the electromagnetic force is only related to the magnitude of the current. Therefore, in order to determine the optimal current, it is necessary to conduct magnetic simulation analysis of the electromagnet.

4.2. Simulation of adsorption capacity

Use Maxwell software to simulate and test the adsorption capacity of the electromagnet, and establish a simulation model as shown in Fig.7. Among them, the magnetic wall surface is set as $10mm$ thick iron plate; The electromagnet uses brass coils with a thickness of $3mm$ inside.

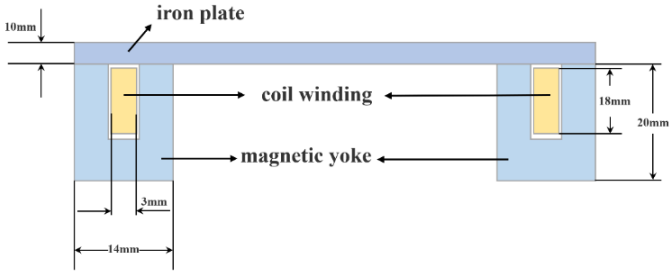

Fig.7 Simulation model of electromagnet

Next, set the coil turns to 2500 ; The magnetic field boundary condition is a balloon shaped boundary, resulting in a magnetic density cloud as shown in Fig.8.

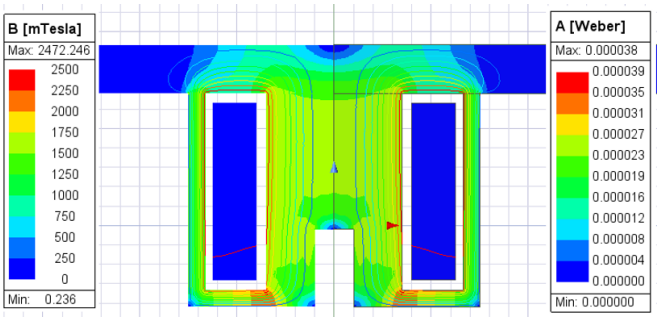

Fig.8 Magnetic density cloud

In order to obtain the influence of different parameters on the adsorption capacity of the electromagnet, the control variable method was used to test the effects of input current and air gap spacing on it, and Figs.9 and 10 are obtained.

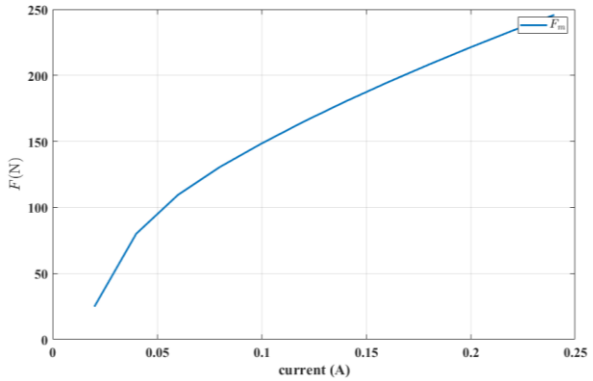

Fig.9 The trend of F_m changing with current

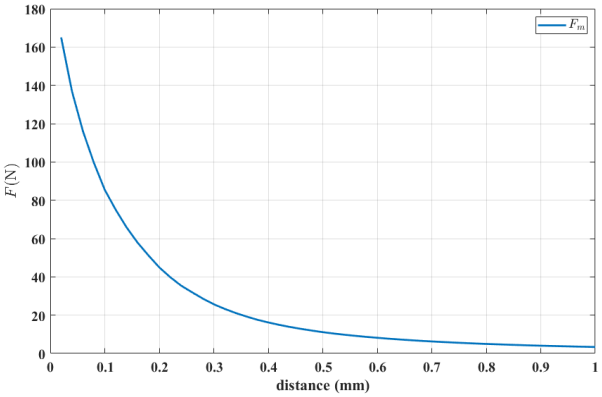

Fig.10 The trend of F_m changing with distance

From Fig.9, it can be seen that the adsorption capacity of the electromagnet is directly proportional to the input current; It should be noted that a larger input current is not necessarily better, as excessive current may cause the walking mechanism to malfunction. Fig.10 shows the trend of the adsorption capacity of the electromagnet with the increase of the air gap spacing. When the air gap spacing is greater than 0.54, the adsorption force $Fm<10N$ of the electromagnet fails.

Based on Fig.9 and 10, when the input current is $0.12A$ and the air gap spacing is $0.02mm$, the adsorption force $Fm=164N$ meets the minimum adsorption force requirement in the safety analysis.

5. Experiment

This section will verify the adsorption force of the electromagnet by building a magnetic testing platform. As shown in Fig.11, attach the electromagnet to the iron plate and connect it to the load cell hook.

Fig.11 Experiment on electromagnetic adsorption force

By setting different input currents and rotating the electromagnet adjustment screw to adjust the air gap spacing, the adsorption force under different parameters was measured using a force gauge, and the results are shown in Fig.12 and Fig.13.

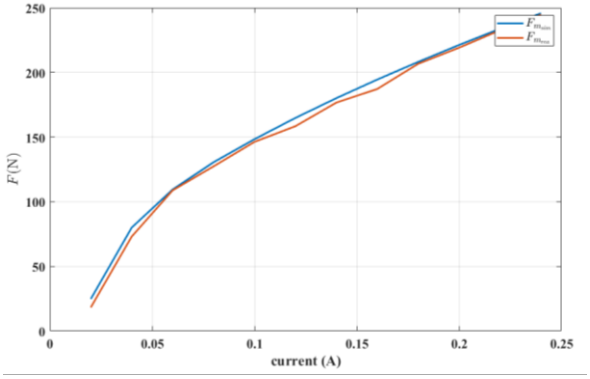

Fig.12 The trend of $F_{m_{rea}}$ changing with current

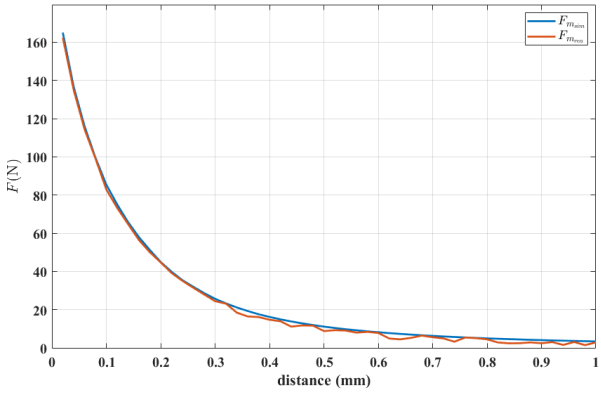

Fig.13 The trend of $F_{m_{rea}}$ changing with distance

The blue solid line in Fig.12 and 13 represent the simulation results, and the red solid line represents the actual measured values. It can be seen that the trend of the actual measured electromagnetic adsorption force is the same as the trend of the simulation results, which verifies the effectiveness of the proposed scheme.

It is worth noting that the simulated data was obtained under ideal conditions, and the actual electromagnetic adsorption capacity may be slightly smaller than the theoretical value. This is why the actual values in the two figs are slightly smaller than the simulated values.

6. Summary

This paper proposed a wheeled walking structure based on electromagnets. On the premise of ensuring mobility, the adhesion ability of ROV to the magnetic wall could be controlled by controlling the electrification of the electromagnet and the input current. In addition, considering safety, combined with mechanical analysis, the minimum adsorption force to ensure the ROV avoids dangerous working conditions, as well as the corresponding input current and air gap spacing parameters of the electromagnet, were obtained. Finally, the reliability of using parameters was verified through a set of experiments.

Acknowledgements

This paper is supported by CNOOC Major Special Projects (Project number: ZX2024ZCCYF1598) and Key R&D Projects of Hainan Province (Project number: ZDYF2023GXJS004).

References

[1] Dalhatu A A, Azevedo R, Udebhulu O D, et al. RECENT DEVELOPMENTS OF REMOTELY OPERATED VEHICLE IN THE OIL AND GAS INDUSTRY[J]. Holos, 2021, 3.

[2] Mazzeo A, Aguzzi J, Calisti M, et al. Marine robotics for deep-sea specimen collection: A systematic review of underwater grippers[J]. Sensors, 2022, 22(2): 648.

[3] Song Y, Wang Z, Li Y, et al. Electrostatic attraction caused by triboelectrification in climbing geckos[J]. Friction, 2022, 10: 44-53.

[4] Santos H B, Teixeira M A S, Dalmedico N, et al. Model predictive torque control for velocity tracking of a four-wheeled climbing robot[J]. Sensors, 2020, 20(24): 7059.

[5] Enjikalayil Abdulkader R, Veerajagadheswar P, Htet Lin N, et al. Sparrow: A magnetic climbing robot for autonomous thickness measurement in ship hull maintenance[J]. Journal of Marine Science and Engineering, 2020, 8(6): 469.

[6] Rezazadegan F, Shojaei K, Sheikholeslam F, et al. A novel approach to 6-DOF adaptive trajectory tracking control of an AUV in the presence of parameter uncertainties[J]. Ocean Engineering, 2015, 107: 246-258.

[7] Do K D, Pan J, Jiang Z P. Robust and adaptive path following for underactuated autonomous underwater vehicles[J]. Ocean Engineering, 2004, 31(16): 1967-1997.

[8] Yoerger D, Slotine J. Robust trajectory control of underwater vehicles[J]. IEEE journal of Oceanic Engineering, 1985, 10(4): 462-470.

[9] Tong S, Li Y. Observer-based fuzzy adaptive control for strict-feedback nonlinear systems[J]. Fuzzy sets and systems, 2009, 160(12): 1749-1764.

[10] Yuh J, Lakshmi R. An intelligent control system for remotely operated vehicles[J]. IEEE Journal of Oceanic Engineering, 1993, 18(1): 55-62.